Experimental verification of reduced intersubband scattering in ordered nanopore lattices

N. L. Dias,[a] A. Garg, U. Reddy, J. D. Young, K. P. Bassett, X. Li, and J. J. Coleman
Department of Electrical and Computer Engineering, University of Illinois, Urbana, Illinois 61801, USA

(Received 23 January 2011; accepted 25 January 2011; published online 18 February 2011)

A photoluminescence study of emission from a periodically perforated quantum well at 77 K is presented. Good agreement is observed between numerical predictions and experimental results. The effects of pore diameter on peak emission wavelength and relative emission from second excited subbands are analyzed. The results are found to be consistent with predictions of reduced intersubband scattering rate in nanopore lattices due to the reduced wave function overlap between the initial and final states arising from the in-plane periodicity. © *2011 American Institute of Physics*. [doi:10.1063/1.3554763]

Low dimensional semiconductor structures are of interest as building blocks for quantum computing and intersubband-based optical devices.[1–4] A necessary requirement for widespread applicability is precise control over spectral properties, which implies the ability to accurately control alloy compositions and geometry at the nanoscale. Three-dimensional (3D) confinement in quantum dots results in δ-function like density of states which leads to high material and differential gain, excellent temperature stability and higher defect and radiation tolerance.[5] Although many of the predicted properties have been experimentally verified, quantum dots have remained limited in their applicability by the limited control in dot positioning and spectral characteristics. Size variations in dot ensembles introduce inhomogeneous broadening effects which cause a deviation from the ideal δ-function like density of states.[6] This coupled with the reduced area fill factor in the active region of quantum dot-based lasers results in increased threshold when compared to quantum well-based laser devices.

The nanopore active layer consists of a quantum well that has been periodically perforated and then filled with a higher bandgap barrier material.[7–9] Electronically, this structure is equivalent to an inverse quantum dot layer in that the lower energy dot regions and the higher energy barriers have been interchanged (Fig. 1). In the limit of small pores or large lattice spacing, the nanopore electronic structure approaches that of a quantum well. At the other extreme of large pores on a small lattice spacing, the nanopore behaves like a quantum dot.[10]

The usefulness of the nanopore active layer lies in the number of degrees of freedom available for defining the electronic structure and hence the spectral properties. The defining parameters of the nanopore are the pore diameter and pitch, the material composition of the low bandgap material and the barrier and the thickness of the active layer. The presence of strain in the InGaAs/GaAs system introduces another parameter that can be used to tailor the emission properties. A comprehensive theoretical analysis of the effect of device geometry and alloy compositions on the band structure of the nanopore lattice has been conducted.[11]

The ability to create a designer band structure makes the nanopore a good candidate for intersubband devices. Lasers fabricated with the nanopore active layer have been shown to lase preferentially at excited states and this has been taken as a sign of reduced intersubband scattering rate relative to a quantum well.[7] Theoretical calculations point to the reduced overlap between wave functions as the primary cause for the reduced intersubband cooling rate.[12]

In this paper, we present for the first time a photoluminescence study of the effect of geometry on the spectral characteristics of a nanopore active layer. The theoretically predicted blue-shift in the spectrum with increasing pore diameter for a constant pitch is experimentally demonstrated. The potential for increased emission from excited states in a nanopore relative to a reference quantum well is presented.

The fabrication process starts with the growth of a 100 nm GaAs buffer layer, followed by a 300 nm $Al_{0.75}Ga_{0.25}As$ carrier confinement layer and a 20 nm GaAs barrier layer. The active region is a 8.7 nm $In_{0.31}Ga_{0.69}As$ quantum well. A 4 nm GaAs cap is then grown to protect the quantum well from damage during subsequent processing steps.

Silicon dioxide is deposited by plasma enhanced chemical vapor deposition. Direct write electron beam lithography is used to define a hexagonal pattern of pores in the polymethyl methacrylate (PMMA). Control over the pore diameter is achieved by varying the electron beam dose from one stripe to the next.

Transfer of the pattern from the PMMA to the oxide is accomplished by a combination of a Freon-based (CHF_3) reactive ion etching (RIE) system and a dilute buffered hydrofluoric acid based wet etch. The need for a dual step oxide

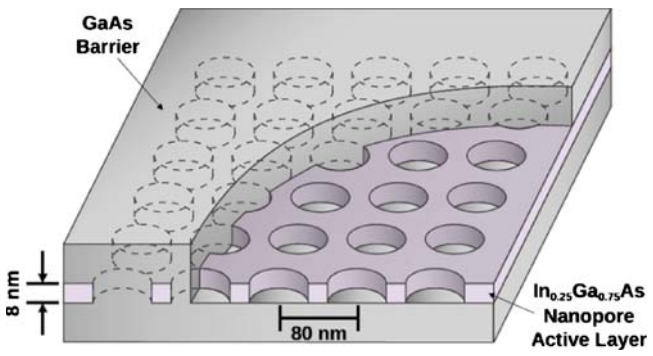

FIG. 1. (Color online) Schematic of nanopore structure consisting of periodically perforated quantum well filled with higher bandgap material.

[a]Electronic mail: ndiasan2@illinois.edu.

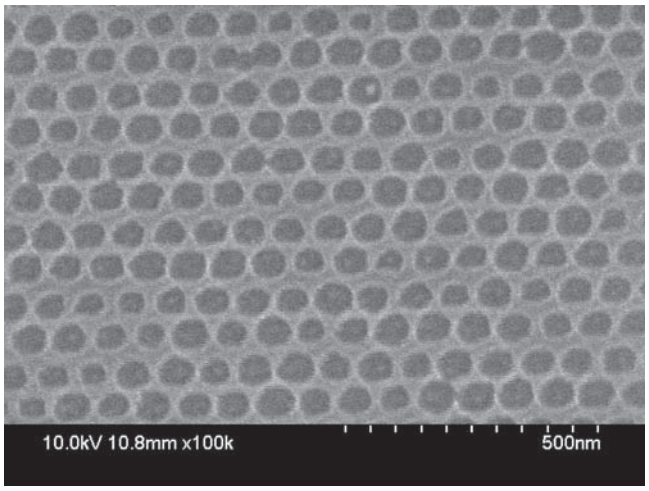

FIG. 2. Secondary-emission monitor image of 80 nm pitch nanopore pattern after wet etching.

etching process arises from the intrinsic porosity of the PMMA film which makes a purely wet etch based process difficult. Also employment of a dry etch only for the pattern transfer results in excessive damage to the substrate severely reducing luminescence efficiency.

The oxide pattern is transferred to the quantum well by a calibrated phosphoric acid:peroxide etch. A scanning electron microscope image of a nanopore pattern with a pitch of 80 nm and an average pore diameter of 60 nm is shown in Fig. 2. After stripping the oxide mask, a 1:10 $NH_4OH:DI$ etch is performed for native oxide removal and the sample is returned to the reactor for regrowth of the upper barrier layers. Liftoff metallization is used to pattern 40 μm $\times 40$ μm apertures at the location of the nanopore patterns.

The CW photoluminescence is obtained using an Ar ion laser emitting at 488 nm. The beam is focused by a microscope objective onto the sample placed in a liquid-N_2 cryostat. The luminescence signal is collected by the same microscope objective, dispersed by a monochromator and detected by a liquid-N_2 cooled Ge detector.

Nanopore patterns with a constant pitch of 80 nm and diameters ranging from 55 to 70 nm were fabricated and measured. Figure 3 shows the peak wavelength and corresponding photon energy as a function of pore diameter. As the pore diameter increases, the nanopore transitions from a quantum well like structure to a quantum dot system. The

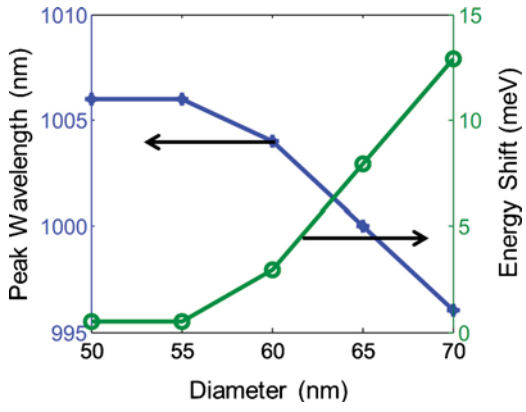

FIG. 3. (Color online) Peak wavelength (energy) versus pore diameter. Peak wavelength blue-shifts with increasing pore diameter.

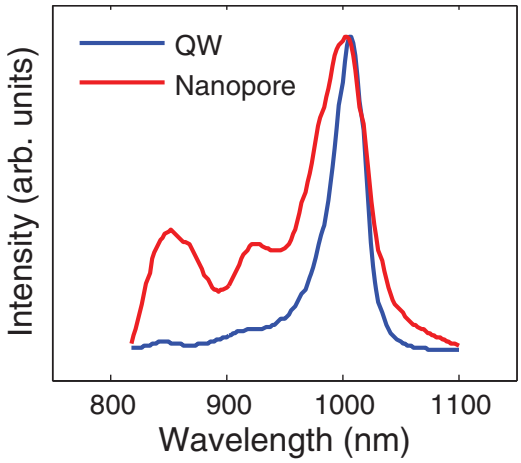

FIG. 4. (Color online) Comparison of photoluminescence emission from etched nanopore and reference quantum well.

effective area of the triangular region formed by three surrounding nanopores decreases with increasing pore diameter. This increasing confinement results in a quadratic increase in ground state energy, which is in agreement with the established theory.[12]

To study the effect of the nanopore on excited state emission, the quantum well was designed to have two interband transitions around 1008 and 928 nm at 77 K. Figure 4 shows the comparison between the normalized photoluminescence from a quantum well and a nanopore pattern with pitch of 80 nm and a pore diameter of 60 nm. Most significantly, the ratio of the emission from the band at 928 nm to the emission at 1008 nm is greater in the nanopore compared to the reference quantum well. The nanopore wave functions can be expressed as

$$\Psi(x,y,z) = \Phi(x,y) \times Z(z),$$

where Φ_{xy} refers to the in-plane variation of the wave function and Z refers to the out-of-plane variation of the wave function. Although the nanopore is not strictly uniform in the z-direction like a quantum well, the variable separation assumption yields accurate results for pore diameters in the 80 nm range. This has been validated by finite element analysis that yields identical bandstructure for a two-dimensional simulation disregarding the z-dimension and a full 3D calculation.

The band at 1008 nm arises from the in-plane subbands formed for the first excited Z-wave function (henceforth denoted as Φ_1) while the band at 928 nm corresponds to the in-plane subbands formed for the second excited Z-wave function (denoted as Φ_2). Electrons in the Φ_2 band can decay in two possible ways: either by relaxation into the Φ_1 band or by direct electron-hole recombination with the corresponding valence subbands. Generally, in quantum wells the interband relaxation processes tend to be very efficient due to phonon scattering, thus limiting the efficiency of emission from the second excited states.

In the nanopore, the in-plane periodicity modifies the Φ_{xy} wave functions. This in-plane variation reduces the overlap between the wave functions thus reducing the probability of transitions from one subband to the next. This has been verified previously in nanopore lasers which exhibit emission from the third Φ_{xy} subband.[7]

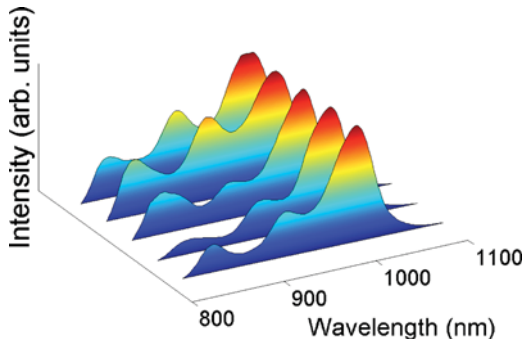

FIG. 5. (Color online) Measured photoluminescence spectra for 80 nm pitch patterns for 50, 55, 60, 65, and 70 nm pore diameters.

As the pattern pitch is varied from 55 to 70 nm keeping the pitch constant at 80 nm, the emission from the Φ_2 band relative to the Φ_1 band increases as shown in Fig. 5. This follows from the tendency of the nanopore to approach quantum dot type behavior as the pore diameter becomes equal to the pitch.

The above measurements for all the nanopore samples were done for a constant pump intensity of 5 kW/cm^2. It should also be noted that the process of performing the nanopore etch results in an effective decrease in the available active gain volume (quantum well). For a 55 nm pore diameter pattern, the remaining InGaAs material is 57% of the original quantum well. This decreases to 30% for a 70 nm pore diameter pattern. Thus the observation of enhanced emission from the Φ_2 band as the pore diameter increases could be an artifact of state filling. However, leakage of carriers into the GaAs barrier for larger pore sizes causes relatively more emission from the barrier layers and counteracts some of the state filling concerns.

We conducted a PL study of the nanopore active layer as a function of device geometry. Evidence of subbands formation by in-plane quantization is observed in spectra taken for wider pore diameters which is in agreement with numerical calculations. Increasing pore diameter leads to increased emission from higher subbands pointing to the reduced scattering rate in the nanopore lattice when compared to a reference quantum well. This is attributed to the reduced overlap between initial and final wave functions due to the in-plane modifications of the quantum well. This ability to tailor both the subband structure and the relaxation rates in the nanopore makes it an ideal candidate for devices based on intersubband transitions.

The authors would like to acknowledge the support of the U.S. Department of Energy, Office of Basic Energy Sciences as part of an Energy Frontier Research Center and the National Science Foundation (Grant No. ECCS 08-21979).

[1]X. Li, Y. Wu, D. Steel, D. Gammon, T. H. Stievater, D. S. Katzer, D. Park, C. Piermarocchi, and L. J. Sham, Science **301**, 809 (2003).
[2]H. Chia-Fu, O. Jeong-Seok, P. Zory, and D. Botez, IEEE J. Sel. Top. Quantum Electron. **6**, 491 (2000).
[3]S. Krishna, P. Bhattacharya, P. J. McCann, and K. Namjou, Electron. Lett. **36**, 1550 (2000).
[4]E.-T. Kim, A. Madhukar, Z. Ye, and J. C. Campbell, Appl. Phys. Lett. **84**, 3277 (2004).
[5]S. Fathpour, Z. Mi, and P. Bhattacharya, J. Phys. D **38**, 2103 (2005).
[6]K. J. Vahala, IEEE J. Quantum Electron. **24**, 523 (1988).
[7]V. C. Elarde and J. J. Coleman, IEEE Photon. Technol. Lett. **20**, 240 (2008).
[8]V. B. Verma, V. C. Elarde, and J. J. Coleman, IEEE J. Quantum Electron. **45**, 10 (2009).
[9]C. Flindt, N. A. Mortensen, and A.-P. Jauho, Nano Lett. **5**, 2515 (2005).
[10]V. B. Verma, N. L. Dias, U. Reddy, K. P. Bassett, X. Li, and J. J. Coleman, Proceedings of the Lasers and Electro-Optics (CLEO) and Quantum Electronics and Laser Science Conference (QELS), 2010.
[11]V. B. Verma and J. J. Coleman, J. Appl. Phys. **105**, 043106 (2009).
[12]V. B. Verma and J. J. Coleman, J. Appl. Phys. **106**, 054503 (2009).